RFI Propagation Paths

J. Richard Fisher

NRAO, Green Bank
rfisher@nrao.edu

Abstract

Protection of radio observatories from RFI from ground-based transmitters generally relies on great circle path diffraction calculations to predict signal strengths at the radio telescopes. However, signal propagation over long distances and over rough terrain is considerably more complex than two-dimensional models assume. This is a brief description of a study of radar signal propagation paths that we have been conducting at Green Bank. Signal reflections from surrounding terrain, aircraft, and rain showers have been observed with extra propagation delays of up to several hundred microseconds and a wide range of directions of arrival. Propagation losses through indirect paths can sometimes be comparable or occasionally less than the great circle path loss. The ranges of delay and directions of arrival have implications for the signal processing requirements of RFI cancellation techniques now under study.

1 Introduction

Recent interest in signal processing techniques for canceling radio frequency interference (RFI) in radio astronomy receivers [1] has prompted us to better understand the properties of signals in frequency bands used for observations with the 100-meter Green Bank Telescope (GBT). One signal of particular interest comes from an FAA air surveillance radar antenna near Bedford, Virginia, about 104 kilometers to the south-southeast of Green Bank, transmitting on the frequencies of 1256 and 1292 MHz. Because of the expansion of the universe, atomic hydrogen radiation at 1420.4 MHz from some distant galaxies is Doppler shifted to the frequencies of this radar. Hence, we would like to find ways of observing this cosmic radiation in the presence of the radar signals.

Our first look at the microsecond time structure of the radar signal received by the GBT showed that the strongest part of each pulse was not at its leading edge as one would expect if the direct great circle path had the lowest path loss. Apparently, an indirect path due to reflections from high terrain was producing a stronger signal from the radar than was the direct path so we set out to understand the propagation modes in more detail. To do this we constructed a bistatic radar map from the received pulse intensity as a function of delay from the direct pulse arrival time and the inferred direction of the sweeping radar beam as described below.

The radar signal is pulsed with a pulse length of 2 microseconds, an average repetition rate of about 340 pulses per second, and a peak transmitted power of several megawatts. The pulse transmission times are jittered by several hundred microseconds in a repeating pattern as described in [2] to resolve distance ambiguities. The radar antenna has a horizontal beam width of 1 degree and rotates about a vertical axis at 5 RPM (12 second sweep period). The forward gain of this antenna is roughly 40 dB, but pulses

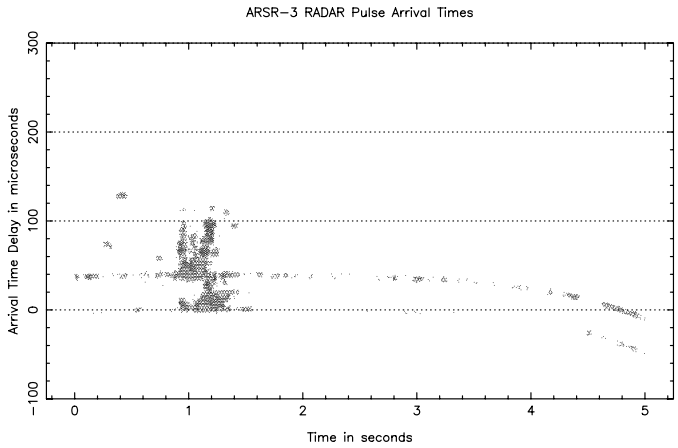

Figure 1: Distribution of measured pulse delays from the inferred direct-path arrival times in data recorded from the GBT. The curvature near the end of the graph is due to sample clock drift that was corrected in the data analysis.

can be seen with the ≈ -15 dBi far sidelobes of the GBT during most of the 12-second sweep from radar antenna sidelobes that probably have an average gain of about -10 dBi. When the radar beam is pointed in the direction of the GBT the induced pulse voltage exceeds the linear range of the GBT receiver for the duration of the pulse, but the receiver recovers immediately after the received pulse voltage falls within its linear range.

2 Terrain Reflection Maps

Figure 1 shows the distribution of measured pulse delays from the direct path arrival time as a function of time from the beginning of the 5-second data stream recorded from the GBT's 1.2-1.7 GHz receiver. Each dot in this figure is a discernible pulse power peak significantly above thermal noise from the receiver. The radar antenna beam passed over the GBT at about 1.3 seconds into this data set. Notice that the biggest cluster of pulses occurs before the radar beam is pointed directly at the telescope and at delays greater than about $40\mu s$. The width of the radar beam in this plot is about 0.033 seconds. The long horizontal stripe of points in Figure 1 is due to a strong reflection at a delay of $40\mu s$ that is visible through the radar antenna sidelobes when it is pointed well away from the radio telescope.

The pulse arrival times shown in Figure 1 may be mapped onto geographic coordinates by assuming that each pulse locus falls on the intersection of three surfaces: the delay ellipsoid with the GBT and the radar antenna at the focii, the vertical plane through the radar beam, and a horizontal plane at the elevation of the GBT. The horizontal plane assumption is not strictly correct since the reflection points are not at the same elevation, but the error is small for delays greater than about $10\mu s$.

Figure 2 shows the same data mapped onto the horizontal plane. The small cluster of points near the top of the map is very likely an aircraft reflection. All other features in this map are due to reflections from high terrain. The heavy cluster of points to

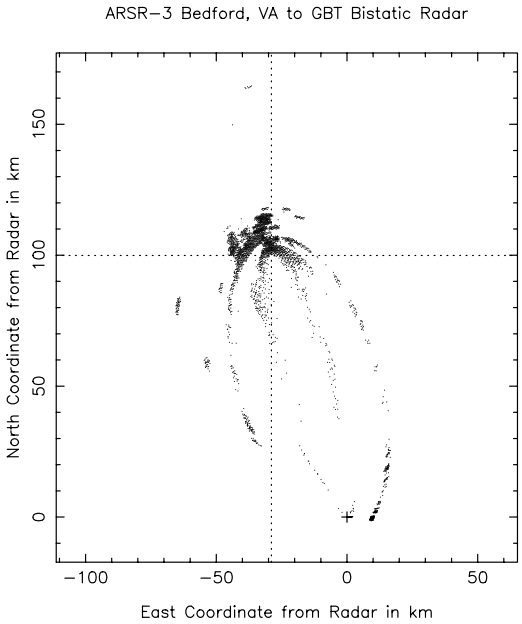

Figure 2: Reflection point locations computed from pulse arrival delays and the radar beam azimuth. The GBT is at the intersection of the two long dotted lines, and the radar is at the small cross near the bottom of the diagram.

the north-west of the GBT is from a high mountain range in this direction. The most prominent ellipse in the map is due to radar antenna sidelobes that are visible from a strong reflection at a high point in the mountains. Each small cluster of points in Figure 2 can be clearly identified with a specific terrain feature on a topographic map overlay to a resolution of a few tenths of a kilometer. In fact, the two free parameters in this data interpretation, the radar beam antenna direction at the beginning of the data set and the direct pulse arrival time offset, were fine tuned by matching many pulse clusters with their terrain counterparts.

3 Differential Delays and Azimuths of Arrival

Nearly all RFI subtraction techniques that might be employed in radio astronomy will need to account for the range of delays and directions of arrival of each signal seen by a radio telescope. Pulse blanking schemes must cover the full delay spread of the arriving pulses. Coherent cancellation techniques must use adaptive filters that can match the delay spread of the multipath propagation. The concept of placing an antenna sidelobe null in the direction of an interfering signal is often too simplistic because the same signal can arrive from many widely spaced directions. Coherent nulling must be done in a combined temporal-spatial domain.

The radar data shown in Figures 1 and 2 can be replotted to show the delay and direction-of-arrival distribution that can be expected for signals with long travel distances in mountainous terrain such as that around the GBT. These plots are shown in

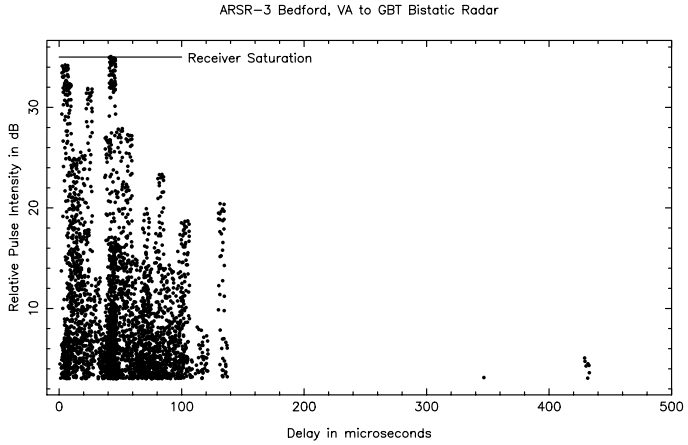

Figure 3: Pulse intensity as a function of delay for the pulses shown in Figures 1 and 2

Figures 3 and 4. Strong terrain reflection delays extend to about $140\mu s$, and the aircraft reflection is at $430\mu s$. The directions of arrival span more than 180^{o}. Each arc in Figure 4 corresponds to one reflection point as the radar beam sweeps over it. Narrow arcs are from distant points, and wide arcs are from points closer to the GBT. Pulses with delays less than $50\mu s$ have been suppressed in Figure 4 because their apparent azimuth spread is artificially large.

4 Aircraft and Rain Shower Reflections

The great circle path and terrain reflections are the dominant propagation paths for RFI from distant sources, but the high sensitivity requirements of radio astronomy can make even high loss paths troublesome. Two of these paths, reflections from aircraft and rain cells, were seen in some other radar data recorded with low-gain antennas at Green Bank. Both are detectable out to delays of at least $800\mu s$. Signals from these two reflection media could be quite strong for periods of time when an aircraft or storm is near the telescope, and cancellation of these reflected signals with adaptive techniques will be challenging because of the rapidly changing amplitudes and delays. We are still working on quantifying the importance of these RFI reflection paths.

Figure 5 shows two gray-scale plots in geographic coordinates relative to the location of the GBT of radar echoes recorded one minute apart. The thin arcs above and to the left of the terrain echoes are echoes from aircraft. The reflections from the aircraft just above center in the top plot is strong enough to show radar antenna sidelobes. In the bottom plot of Figure 5 you can see that all of the aircraft echoes have moved or disappeared, and one or two new ones have appeared. It is hard to follow the motion of individual echoes with just two plots, but a series of five such maps shows the tracks of about ten aircraft in the area plotted.

On one of the days that we recorded data from this radar there happened to be rain showers in the area. Figure 6 shows two radar maps recorded six minutes apart which show diffuse echoes from five or six rain cells to the north of the GBT. By comparing the two maps you can see that in the six minutes between them the northern-most cells

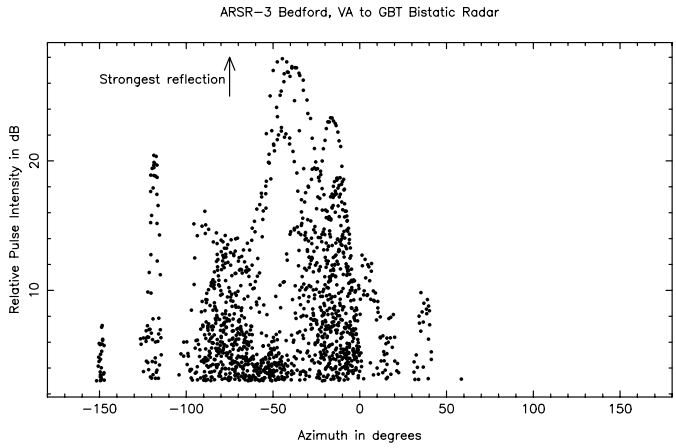

Figure 4: Pulse intensity as a function of inferred azimuth of the radar pulse reflection point for pulses with delays greater than 50 microseconds. Zero azimuth is due North and +90 degrees is due East as seen from the GBT.

have dissipated, and a strong new cell has appeared closer and to the north-west of the GBT.

Of course, a great deal is known about radar echoes from aircraft and rain showers so there is nothing terribly new in these data. However, they do point out that the business of RFI mitigation with signal processing techniques is more complex than one might think. Substantial progress in this field is going to require parallel studies of intrinsic signal characteristics, long distance propagation effects, and sophisticated signal processing techniques.

References

[1] Fridman, P. A., & Baan, W. A., 2001, "RFI Mitigation Methods in Radio Astronomy," Astron. & Astrophys., 378, 327.

[2] Fisher, Rick, 2001, "Analysis of Radar Data from February 6, 2001," http://www.gb.nrao.edu/~rfisher/Radar/analysis.html

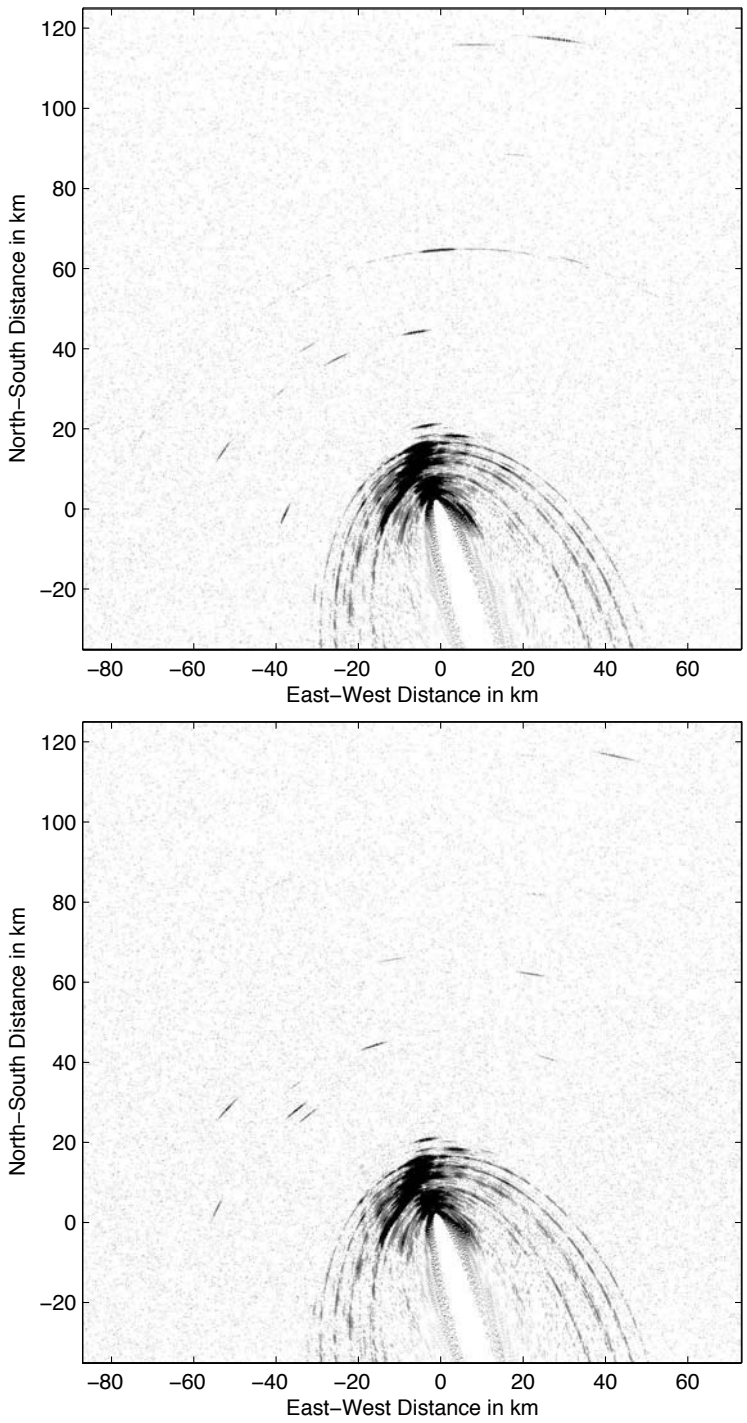

Figure 5: Radar echoes plotted in geographic coordinates relative to the GBT. The display on the top was recorded one minute earlier than the one at the bottom. Arcs that move or appear on only one display are echoes from aircraft.

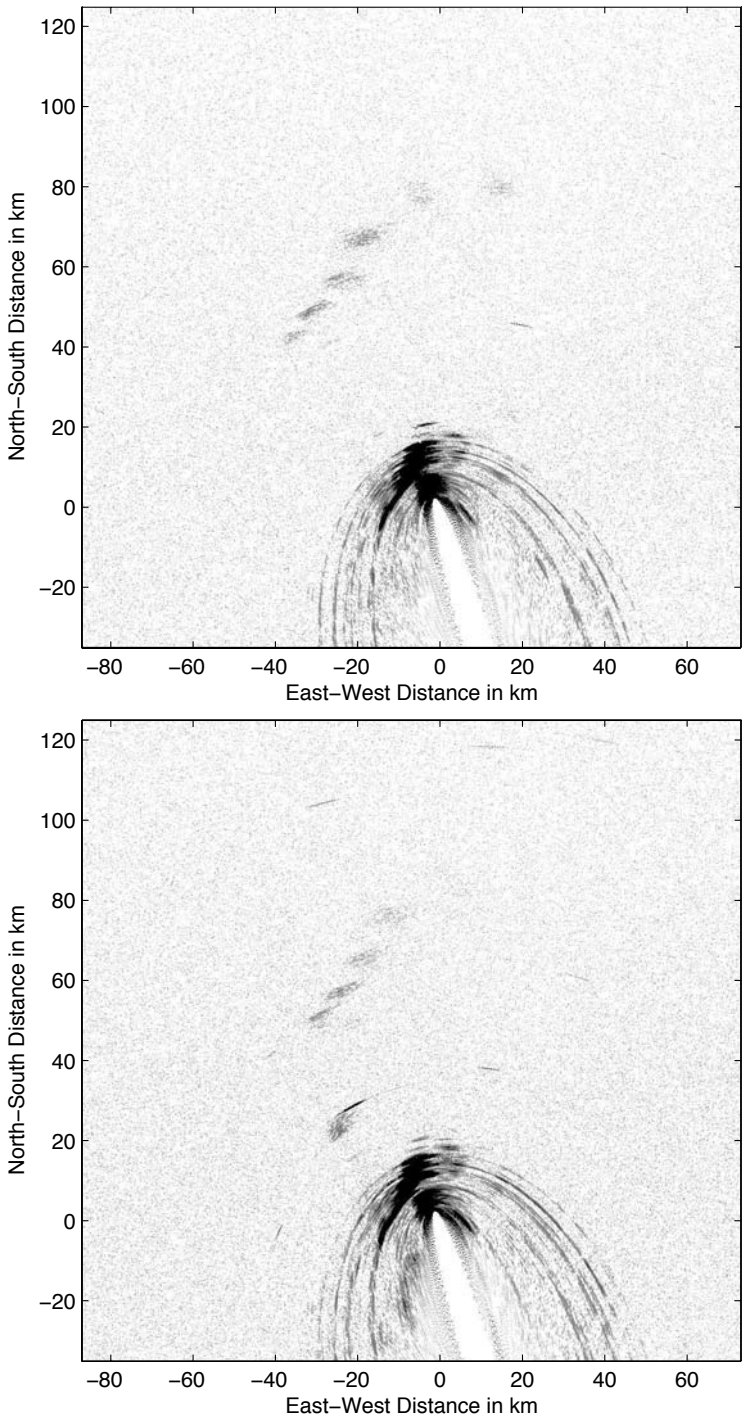

Figure 6: Radar echoes plotted in geographic coordinates relative to the GBT. The display on the top was recorded six minutes earlier than the one at the bottom. The diffuse echoes near the center of the maps are rain showers.